Design and Synthesis of Potent and Selective α4β7 Integrin Antagonists

Jürgen Boer,[†] Dirk Gottschling,[†] Anja Schuster,[‡] Monika Semmrich,[‡] Bernhard Holzmann,*,[‡,§] and Horst Kessler*,[†,§]

Institut für Organische Chemie und Biochemie, Technische Universität München, Lichtenbergstrasse 4, D-85747 Garching, Germany, and Institut für Medizinische Mikrobiologie, Immunologie und Hygiene, Technische Universität München, Trogerstrasse 4a, D-81675 München, Germany

Received December 28, 2000

Interactions of the integrins α4β7 with its cognate ligand mucosal addressin cell adhesion molecule-1 (MAdCAM-1) play a crucial role in the development of mucosa-associated lymphoid organs, in the generation of mucosal immune responses, and in diverse pathological processes such as chronic inflammatory bowel disease and type I diabetes. Using a previously developed spatial screening technique we describe the development of potent and selective α4β7 integrin antagonists based on the domain 1 Leu-Asp-Thr (LDT) sequence of MAdCAM-1 that is essential for α4β7 integrin binding. A library of homodetic cyclic penta- and hexapeptides was synthesized presenting the pharmacophoric LDT-sequence in different conformations. The cyclic hexapeptide **P10** *cyclo*(Leu-Asp-Thr-Ala-D-Pro-Ala) inhibits α4β7 integrin mediated cell adhesion to MAdCAM-1 effectively. Further optimization of the lead structure **P10** resulted in cyclic hexapeptides with enhanced activity. The compounds **P25** *cyclo*(Leu-Asp-Thr-Ala-D-Pro-Phe), **P28** *cyclo*(Leu-Asp-Thr-Asp-D-Pro-Phe), **P29** cyclo(Leu-Asp-Thr-Asp-D-Pro-His), and **P30** *cyclo*(Leu-Asp-Thr-Asp-D-Pro-Tyr) strongly inhibited α4β7 integrin mediated cell adhesion to MAdCAM-1, but they did not affect binding of the closely related α4β1 integrin to VCAM-1.

Introduction

Integrins are heterodimeric transmembrane glycoproteins consisting of one α and one β subunit. They are involved in cell−cell and cell−matrix interactions.[1] At present, the existence of 15 different α and β subunits are assured composing 23 different known integrin receptors.[2] The family of the integrins shows tremendous differences in their biological function and ligand specifity. We focused on α4β7 integrins which form together with α4β1 the group of the α4 integrins. Both receptors are expressed on most leukocyte cell types and mediate as leukocyte receptors cell−cell as well as cell−matrix interactions. The most important endogenous ligands for α4 integrins are the vascular cell adhesion molecule-1 (VCAM-1) and fibronectin (Fn).[3,4] Mucosal addressin cell adhesion molecule-1 (MAdCAM-1) is under physiological conditions an exclusive counter receptor for α4β7 integrins.[5,6]

MAdCAM-1, like VCAM-1, belongs to the immunoglobulin superfamily (IgSF) and possesses three immunoglobulin like domains (Ig-domains). A carbohydrate rich mucin like domain is inserted between the second and the third Ig-domains. Binding of α4β7 integrins to MAdCAM-1 is mediated primarily by the first N-terminal Ig-domain, but sequences in the second Ig-domain are also involved. Peptide epitope mapping and site-directed mutagenesis studies on MAdCAM-1 indicated that the Leu-Asp-Thr (LDT) motif present in the N-terminal Ig-domain is required for binding to α4β7 integrins.[7−9] The LDT motif is located within the C−D loop of the first Ig-domain.

MAdCAM-1 is the dominating counter receptor for α4β7 integrins on mucosal endothel cells.[5,10] Organ specific adhesion of normal lymphocytes and lymphoma cells to high endothelial venules of Peyer's patches is mediated by α4β7 integrins.[11−13] In mouse models it was demonstrated that antibodies specific for β7 integrins and/or MAdCAM-1 block recruitment of lymphocytes to inflamed colon and reduce significantly the severity of colonic inflammatory disease.[14] Moreover, antibodies against β7 integrins protected mice from the development of insulin-dependent diabetes.[15] Therefore, the α4β7/MAdCAM-1 adhesions pathway represents a potent and organ specific target for therapeutic modulation of inflammatory diseases of the gastrointestinal tract and autoimmune diabetes.

We report here the design, synthesis, and biological evaluation of conformationally restricted cyclic peptides that target the α4β7/MAdCAM-1 interaction based on the known LDT motif. For the development of potent and selective α4β7 integrin antagonists, it is of crucial importance to determine the bioactive conformation of the binding motif in MAdCAM-1.[16−18] We have previously demonstrated that libraries of stereoisomeric constrained cyclic peptides are particularly suitable for defining the optimal conformation required for binding to a receptor.[16,18−21] Therefore, to elucidate the bioactive conformation of the LDT binding motif, a library

* Address for correspondence. Prof. Dr. H. Kessler: Institut für Organische Chemie und Biochemie der Technischen Universität München, Lichtenbergstrasse 4, D-85747 Garching, Germany; tel, ++49-89-289 13301; fax, ++49-89-289 13210; e-mail, Kessler@ch.tum.de. Prof. Dr. B. Holzmann: Institut für Medizinische Mikrobiologie, Immunologie und Hygiene der Technischen Universität München, Trogerstrasse 4a, D-81675 München, Germany; tel, ++49-89-4140 2033; fax, ++49-89-4140 4868; e-mail, holzmann@nt1.chir.med.tu-muenchen.de.

§ These authors contributed equally to this work.
† Institut für Organische Chemie und Biochemie.
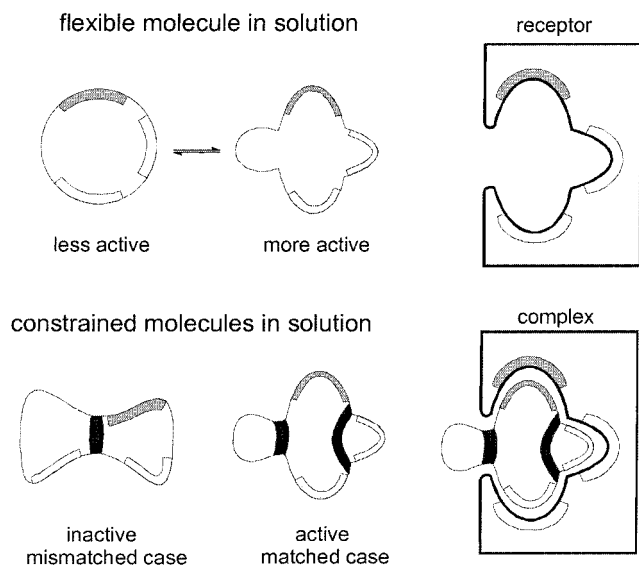‡ Institut für Medizinische Mikrobiologie, Immunologie und Hygiene.

Figure 1. Influence of the conformational restrictions induced by cyclization leading to potent active compounds (matched case) or inactive compounds (mismatched case).

containing constrained homodetic cyclic peptides was synthesized.

Principles of Peptide Design

Peptide backbone cyclization leads to a drastic reduction of conformational space available in solution. The constrained compounds, if active, indicate a structure of the binding motif more closely related to the receptor bound peptide conformation than the corresponding linear sequences (matched case).[17−19] If conformational restriction forces the pharmacophoric motif in conformations not related to the active structure, it leads to peptides with drastically reduced activity or being completely inactive (mismatched case) (Figure 1).

We focused our design on homodetic cyclic penta- and hexapeptides, because larger ring size exhibits greater flexibility. In the case of homodetic cyclic peptides, the backbone conformation depends strongly on the configuration of the amino acid residues. Interactions of the functional groups of the side chains with the peptide backbone are less important.[16,22,23] The knowledge about the conformational behavior in dependency on the configuration of the amino acids can be utilized for a template orientated drug design. A systematic scan of the conformational space can be performed by a controlled insertion of structure inducing amino acids (spatial screening).[16,18,19] Therefore, our group intensively investigated the solution structures of cyclic penta- and hexapeptides containing L-alanine and D-alanine as well as L- and D-proline as structure inducing amino acids by NMR spectroscopy and molecular dynamic (MD) calculations.[24,25]

Results and Discussion

Development of a Lead Structure. At first, we started our spatial screening by synthesizing five cyclic pentapeptides with the sequence *cyclo*(Leu-Asp-Thr-Ala-Ala) in which each amino acid is once in the D-conformation. However, instead of D-alanine we used D-proline since it is known that D-proline has a very strong structurally inducing effect.[16] In this way, we
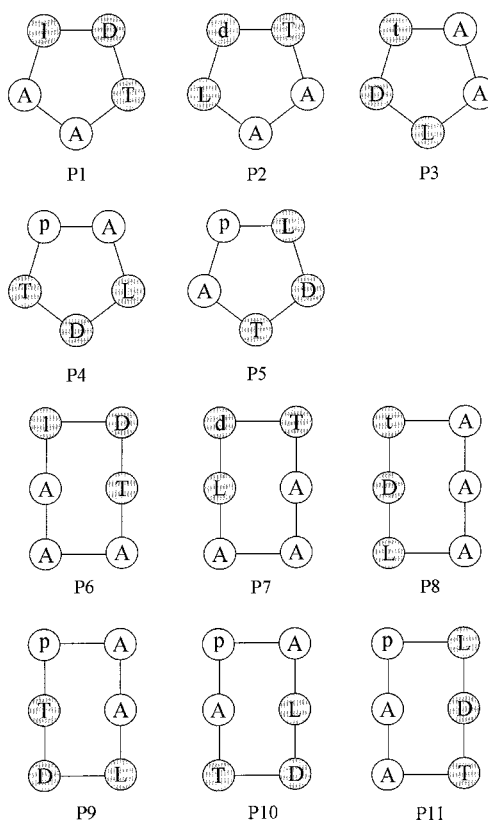

Figure 2. Arrangement of the bioactive LDT motif in cyclic penta- and hexapeptides with one structure inducing amino acid (D-amino acid). The homodetic cyclic hexapeptides normally prefer a conformation with two facing β-turns. In addition, the D-amino acids and especially D-proline prefer the $i + 1$ position of a βII′-turn.

obtained the cyclic pentapeptides **P1**−**P5**. At second, we used the same approach for the hexapeptide *cyclo*(Leu-Asp-Thr-Ala-Ala-Ala), yielding the six compounds **P6**−**P11** (Figure 2).

As we know from structures derived from model peptides such as *cyclo*(d-Pro-Ala$_4$), *cyclo*(d-Ala-Ala$_4$), *cyclo*(d-Pro-Ala$_5$), and *cyclo*(d-Ala-Ala$_5$), the pharmacophoric LDT amino acid sequence is presented in the 11 cyclic peptides **P1** − **P11** in distinctly different conformations.[24,26] According to our models, two facing β-turns are induced in cyclic hexapeptides containing a D-amino acid and no other structure inducing amino acids: a βII′-turn in which the D-amino acid occupies the $i+1$ position and a facing β-turn in equilibrium between βI- and βII-types. Also in the pentapeptides containing only one D-amino acid as structure inducing amino acids, the D-amino acid occupies the $i+1$ position of a βII′-turn. However, the facing site exhibits flexibility and shows several conformational families.[26]

For our peptide library we expected a large spatial screening in the biological assays. The cyclic peptides were tested for their ability to inhibit adhesion of $\alpha_4\beta_7$ integrin expressing 38-β7 lymphoma cells to chinese hamster ovary (CHO) cells stably transfected with MAdCAM-1. The results are summerized in Table 1.

Only the two hexapeptides **P10** and **P11** inhibited binding of $\alpha_4\beta_7$ integrins to MAdCAM-1 effectively in our assays. Compound **P10** showed higher activity compared with **P11**. The linear precursor of the cyclic hexapeptide **P10** H$_2$N-Leu-Asp-Thr-Ala-D-Pro-Ala-OH

Table 1. Effect of Cyclic Peptides on 38-β7 Lymphoma Cell Binding to CHO-MAdCAM-1 Cells[a]

	compound	adhesion [%]
P1	*cyclo*(**l**-D-T-A-A)	100
P2	*cyclo*(**l**-**d**-T-A-A)	137
P3	*cyclo*(L-D-**t**-A-A)	85
P4	*cyclo*(L-D-T-**p**-A)	89
P5	*cyclo*(L-D-T-A-**p**)	74
P6	*cyclo*(**l**-D-T-A-A)	63
P7	*cyclo*(L-**d**-T-A-A-A)	85
P8	*cyclo*(L-D-**t**-A-A-A)	nt[b]
P9	*cyclo*(L-D-T-**p**-A-A)	111
P10	*cyclo*(L-D-T-A-**p**-A)	7
P11	*cyclo*(L-D-T-A-A-**p**)	30

[a] Cell adhesion is presented as a percentage of medium control. Peptides were used at 1 mg/mL. The data represent the mean of two independent experiments. [b] nt, not tested (peptide P8 was not soluble).

showed no activity even with a concentration of 2 mg/mL peptide (not listed in Table 1).

The results of our spacial screening suggest that the conformation of the LDT motif in the active peptides **P10** and **P11** closely resembles the receptor bound conformation. The lack of activity of the linear sequence of the cyclic hexapeptide **P10** emphasizes that the activity of the cyclic analogue derived from a conformational effect. Our pentacyclic compounds **P1**−**P5** seem to present the pharmacophoric motif not in active conformation; however, their higher flexibiltity[26] compared with the hexapeptides is a possible explanation for their low receptor affinity. Therefore, we chose the most active cyclic peptide **P10** as lead structure for further optimizations.

On the basis of these results, a structure prediction of our lead structure **P10** and of analogue peptide sequences is possible. In the bioactive conformation, the LDT motif is arranged in a β-turn with the aspartic acid in the *i+1* position or at least the bioactive conformation can be reached easily starting from this conformation.

Optimization of the Lead Structure. Knowing the optimal backbone conformation of the tripeptide LDT, we systematically optimized each amino acid residue in **P10** (Table 2) retaining the configuration of all the residues (SAR under conformational control).[27] Since we were searching for integrin antagonists with increased activity, we changed the sensitivity of our biological test system in order to facilitate a differentiation between highly potent compounds. In these experiments, the biological activity was determined by inhibition of 38-β7 lymphoma cell adhesion to immobilized MAdCAM-

Ig fusion protein. As compared to the use of CHO-MAdCAM-1 transfectants as a substrate, coating of plates with the MAdCAM-Ig protein yields a higher ligand density and results in more stringent conditions for the selection of bioactive compounds. Therefore, inhibition of 38-β7 cell adhesion to MAdCAM-Ig with 1 mg/mL of the inhibitor **P10** was less efficient than inhibition of binding to CHO-MAdCAM-1 (38% residual adhesion for MAdCAM-Ig versus 7% for CHO-MAdCAM-1 cells; Tables 1 and 2).

Modifications within the LDT motif of peptide **P10** were carried out using functionally related amino acids. Leucine (**P10** and **P18**) was replaced by valine (**P13**), isoleucine (**P14**), phenylalanine (**P20**), D- and L-phenylglycine (**P21** and **P22**), and also by glycine (**P12**). Threonine (**P10** and **P18**) was substituted by glycine (**P15**), serine (**P16**), and valine (**P17** and **P19**). The peptides were tested for their ability to inhibit the $\alpha_4\beta_7$ integrin-dependent cell binding to MAdCAM-1 (Table 2). The substitution of leucine by glycine (**P12**), valine (**P13**), phenylalanine (**P20**), or D- and L-phenylglycine (**P21** and **P22**) led to inactive compounds. These results confirm the essential role of the amino acid residue leucine of the LDT motif for binding to $\alpha_4\beta_7$ integrins.

The exchange of threonine by glycine (**P15**) and serine (**P16**) resulted in inactive compounds. However, the valine modifications (**P17** and **P19**) showed activity in the same order of magnitude as the corresponding parental peptides (**P10** and **P18**). This result is consistent with previous reports showing the LDV sequence represents a binding motif for α_4 integrins in fibronectin.[28,29] Accordingly, the threonine hydroxyl function seems not to contribute to the binding of the LDT peptides to $\alpha_4\beta_7$ integrins.

The importance of the amino acids in positions 4 to 6 in **P10** *cyclo*(Leu[1]-Asp[2]-Thr[3]-Ala[4]-D-Pro[5]-Ala[6]) was also checked by systematic variation. Alanine at position 6 was successively replaced by acidic (aspartic acide, glutamic acid) basic (arginine), aromatic (phenylalanine, tyrosine, histidine) residues as well as by threonine and methionine. In addition, the nonnatural hydrophobic amino acids benzoylphenylalanine (Bpa), cyclohexylglycine (Chg), and tetrahydroisoquinoline-3-carboxylic acid (Tic) were also used.

The substitution of alanine at position 6 by aspartic (**P23**) and glutamic acid (**P24**) resulted in a loss of activity. This finding was further corroborated by the

Table 2. Effect of Cyclic Peptides on 38-β7 Lymphoma Cell Binding to MAdCAM-Ig[a]

	compound	adhesion [%]		compound	adhesion [%]
P12	*cyclo*(**G**-D-T-A-p-A)	105 ± 5	**P29**	*cyclo*(L-D-T-**D**-p-**H**)	9 ± 10
P13	*cyclo*(**V**-D-T-A-p-A)	97 ± 10	**P30**	*cyclo*(L-D-T-**D**-p-**Y**)	3 ± 4
P14	*cyclo*(**I**-D-T-A-p-A)	64 ± 35	**P31**	*cyclo*(L-D-T-**D**-p-**M**)	15 ± 17
P15	*cyclo*(L-D-**G**-A-p-A)	91 ± 17	**P32**	*cyclo*(L-D-T-**D**-p-**Bpa**)	10 ± 1
P16	*cyclo*(L-D-**S**-A-p-A)	90 ± 7	**P33**	*cyclo*(L-D-T-**D**-p-**Chg**)	58 ± 2
P17	*cyclo*(L-D-**V**-A-p-A)	50 ± 23	**P34**	*cyclo*(L-D-T-**D**-p-**Tic**)	9 ± 1
P18	*cyclo*(L-D-T-**p**-A)	47 ± 5	**P35**	*cyclo*(L-D-T-**D**-**f**-A)	63 ± 16
P19	*cyclo*(L-D-**V**-**D**-p-A)	40 ± 7	**P36**	*cyclo*(L-D-T-**D**-**f**-**F**)	56 ± 54
P20	*cyclo*(**F**-D-T-**D**-p-A)	102 ± 8	**P37**	*cyclo*(L-D-T-A-**d**-**D**)	99 ± 6
P21	*cyclo*(**Phg**-D-T-**D**-p-A)	98 ± 9	**P38**	*cyclo*(L-D-T-A-**f**-**D**)	86 ± 12
P22	*cyclo*(**phg**-D-T-**D**-p-A)	114 ± 20	**P39**	*cyclo*(L-D-T-**K**-p-**F**)	85 ± 21
P23	*cyclo*(L-D-T-A-p-**D**)	115 ± 13	**P40**	*cyclo*(L-D-T-**K**-p-**D**)	102 ± 4
P24	*cyclo*(L-D-T-A-p-**E**)	65 ± 4	**P41**	*cyclo*(L-D-T-**K**-p-**Y**)	81 ± 4
P25	*cyclo*(L-D-T-A-p-**F**)	7 ± 3	**P42**	*cyclo*(L-D-T-**M**-p-**D**)	83 ± 14
P26	*cyclo*(L-D-T-A-p-**R**)	26 ± 3	**P43**	*cyclo*(L-D-T-**W**-p-**D**)	87 ± 14
P27	*cyclo*(L-D-T-A-p-**T**)	49 ± 24	**P44**	*cyclo*(L-D-T-**Y**-p-**D**)	76 ± 25
P28	*cyclo*(L-D-T-**D**-p-**F**)	3 ± 4	**P45**	*cyclo*(L-D-T-**F**-p-**D**)	100 ± 10

[a] Cell adhesion is presented as a percentage of medium control. Peptides were used at 1 mg/mL. The data represent the mean ± SD of at least three independent experiments.

Table 3. PBL Adhesion Cells to Laminin in the Presence of Cyclic Peptides

	compound	adhesion [%]
P28	*cyclo*(L-D-T-D-p-**F**)	95 ± 21
P29	*cyclo*(L-D-T-D-p-**H**)	114 ± 16
P30	*cyclo*(L-D-T-D-p-**Y**)	111 ± 15
P31	*cyclo*(L-D-T-D-p-**M**)	102 ± 16

[a] Cell adhesion is presented as a percentage of medium control. Peptides were used at 1 mg/mL. The data represent the mean ± SD of at least three independent experiments.

low inhibitory effect of the peptides **P37**, **P38**, **P42**–**P45**. In contrast, the replacement of alanine by the aromatic amino acid residues phenylalanine (**P25** and **P28**), tyrosine (**P30**), histidine (**P29**), Bpa (**P32**), or Tic (**P34**) strongly enhanced activity. These results are in accordance with the assumption that a hydrophobic interaction supports binding of these peptides to the integrin receptor. Moreover, compounds with methionine (**P31**) and arginine (**P26**) substitutions show increased activity. Peptides containing threonine (**P27**) and Chg (**P33**) at position 6 show activities similar to those of the parental molecules.

The replacement of D-proline (**P18**) at position 5 by D-phenylalanine (**P35**) had no influence of the ability of this compound to inhibit the α$_4$β$_7$ integrin/MAdCAM-1 interaction. Accordingly, the D-amino acid is not directly involved in the binding to the integrin receptor. Its function is exclusively to induce the active conformation of the pharmacophoric residues. Therefore this position is free for further manipulations such as linking to fluorescence dye or dimerization.

Substitution of alanine at position 4 for aspartic acid did not affect the inhibitory properties of the compounds (**P10**–**P18**, **P17**–**P19**, and **P25**–**P28**). However, the presence of lysine (**P39**–**P41**) substantially decreased the activity of the highly active antagonists **P25**, **P28**, and **P30**.

Selectivity of Compounds for α$_4$β$_7$ **Integrin.** In addition to biological activity, selectivity is a major goal in drug development. Previous work has shown that the concept of conformational constrain induced in cyclic peptides is also valuable for the development of highly selective integrin antagonists.[16,30]

In a first set of experiments, we examined the influence of the peptides **P28**–**P31** on the binding of human peripheral blood lymphocytes (PBL) to laminin. This interaction is mostly mediated by integrin α$_6$β$_1$. The results demonstrate that all compounds tested did not affect α$_6$β$_1$-dependent PBL adhesion to laminin (Table 3). Control experiments indicated that binding of PBL to MAdCAM-Ig was strongly inhibited by these compounds (data not shown).

To further define the selectivity, the ability of these peptides to inhibit interactions of integrins with their cognate ligands, binding of α$_4$β$_7$, and interactions of the structurally related integrin α$_4$β$_1$ to VCAM-1 was investigated. Adhesion mediated by α$_4$β$_1$ integrin was tested using Jurkat (α$_4$β$_1$⁺, α$_4$β$_7$⁻) lymphoma cells. Our results show that α$_4$β$_7$/VCAM-1 interactions were also inhibited by peptides **P25** and **P28**–**31**, although with markedly lower efficacy than α$_4$β$_7$ binding to MAdCAM-1. In contrast, the cyclic peptides did not affect adhesion of α$_4$β$_1$ to VCAM-1 (**P25**, **P28**, and **P31**) or had very weak inhibitory activity (**P29** and **P30**). The inhibitory activities of **P28**–**P30** for α$_4$β$_1$ mediated cell adhesion

Table 4. Specific Effects of Cyclic Peptides on Integrin α$_4$β$_7$ and α$_4$β$_1$ Mediated Cell Adhesion to MAdCAM-Ig and VCAM-1[a]

compound	α4β7/MAdCAM adhesion [%]	α4β7/VCAM adhesion [%]	α4β1/VCAM adhesion [%]
P25 *cyclo*(L-D-T-A-p-F)	7 ± 3	36 ± 7	109 ± 20
P28 *cyclo*(L-D-T-D-p-F)	3 ± 4	38 ± 20	72 ± 10
P29 *cyclo*(L-D-T-D-p-H)	9 ± 10	27 ± 14	74 ± 16
P30 *cyclo*(L-D-T-D-p-Y)	3 ± 4	37 ± 13	78 ± 3
P31 *cyclo*(L-D-T-D-p-M)	15 ± 17	36 ± 12	108 ± 18
P46 *cyclo*(N-E-h-F-G)	100 ± 0	93 ± 19	nt[b]

[a] Cell adhesion is presented as a percentage of medium control. Peptides were used at 1 mg/mL. The data represent the mean ± SD of at least three independent experiments. [a] nt, not tested.
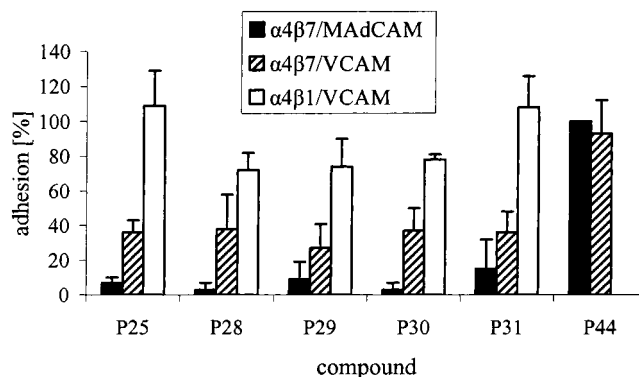
Figure 3. Binding of 38-β7 lymphoma cells (α$_4$β$_7$) and Jurkat cells (α$_4$β$_1$) after incubation with cyclic peptides to immobilized VCAM-1 and MAdCAM-Ig. The results are shown as mean ± standard deviation.

to VCAM-1 were, however, considerably lower than for α$_4$β$_7$/MAdCAM-1 interactions. The negative control peptide **P46** did not have any inhibitory effect. The results are summarized in Table 4 and Figure 3.

NMR and Molecular Modeling. The structure prediction of our active peptides with two facing β-turns with D-proline at the *i* + 1 position of a βII′-turn and the aspartic acid at the *i* + *1* position of a βI- or βII-turn is confirmed by NMR data. In the ROESY spectrum acquired in DMSO at 300 K of the compound **P25**, one of our most potent and selective α$_4$β$_7$ integrin antagonists, all sequential Hα(*i*)-NH(*i*+1) connectivities confirm the trans configuration of the amide bonds. No Hα(*i*)-Hα(*i*+1) connectivities for cis amide bond can be assigned. Moreover, the characteristic ROE connectivities between Hα(*i*)-NH(*i*+2) for β-turns between D-Pro⁵Hα and Leu¹NH as well as between Asp²Hα and Ala⁴NH are observed in the ROESY spectrum of peptide **P25**.

The three-dimensional structure of compound **P25** in DMSO was successively determined by metric matrix distance geometry (DG) and molecular dynamics (MD) simulations. Interresidual distance constraints involving backbone protons are shown in Table 5.

The structure reported in Figure 4, based on DG and MD calculations, fulfills all reported constraints. D-Pro occupies the *i* + *1* position of a βII′-turn, and the second β-turn with the aspartic acid in the *i* + *1* position shows a strong tendency toward a βI-type. The superpositions with ideal βII′- and βI-turns using the trace (Cα) of the four residues involved in the turns show good fits with root-mean-square deviations (RMSD) values of 0.2 and 0.5, respectively. The temperature dependence of backbone amide protons (Table 6) shows the expected low coefficient values for the amino acids at positions 1 and 4. The low temperature dependence of the threonine NH
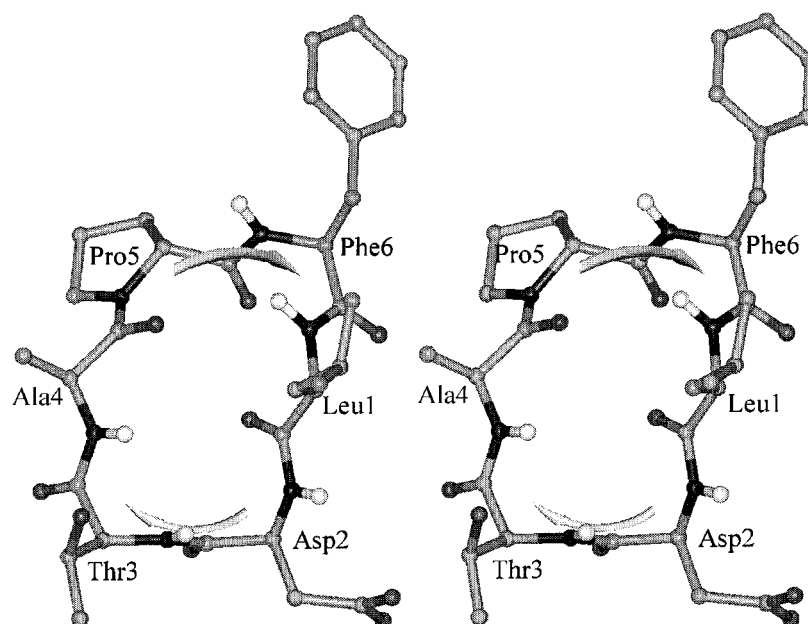
Figure 4. Stereoview of the energy minimized structure determined for peptide **P25** using constrained DG and MD simulations. The two arrows indicate the direction of the hydrogen bonds of the two facing β-turns from the carbonyl group of the residue in the *i* position to the amide group of the residue in the *i* + 3 position.

Table 5. Interresidual Distance Constraints Involving Backbone Protons of Compound **P25**

proton 1	proton 2	lower bound [Å]	upper bound [Å]
LEU^1 H$^\alpha$	ASP^2 H^N	2.22	2.72
LEU^1 H^N	PRO^5 H$^\alpha$	3.39	4.15
LEU^1 H^N	PHE^6 H$^\alpha$	3.31	4.04
LEU^1 H^N	PHE^6 H^N	2.86	3.50
LEU^1 H^N	ALA^4 H^N	4.83	5.90
ASP^2 H$^\alpha$	THR^3 H^N	3.15	3.85
ASP^2 H^N	THR^3 H^N	3.02	3.69
THR^3 H$^\alpha$	ALA^4 H^N	3.04	3.72
THR^3 H^N	ALA^4 H^N	2.94	3.59
PRO^5 H$^\alpha$	PHE^6 H^N	1.93	2.36
ALA^4 H^N	ASP^2 H$^\alpha$	4.44	5.32

Table 6. Temperature Dependence of the Amide Proton Chemical Shift of **P25** in DMSO^a

	Leu^1	Asp^2	Thr^3	Ala^4	Phe^6
P25	2.6	4.6	−0.2	−3.0	6.2

^{a} The coefficients are given in $-\Delta\delta/\Delta T$ [ppb/K] (parts per billion per K).

signal in position 3 might be explained with the presence of a hydrogen bond to threonine hydroxyl group or steric shielding.

Interestingly, in the X-ray structure of MAdCAM-1,[31] the pharmacophoric LDT motif found in the C−D loop of the first Ig-domain does not fold in a β-turn. However, the superposition of the LDT sequence found in crystal structure of MAdCAM-1 and in our active structure **P25** matches very well (RMSD = 0.5) except for the orientation of the amide bond between Leu and Asp (Figure 5).

Conclusions

The use of cyclic peptides to constrain the LDT motif in defined conformations (spatial screening) has led to the identification of the cyclic hexapeptide **P10** *cyclo*-(Leu-Asp-Thr-Ala-D-Pro-Ala) which is an inhibitor of the MAdCAM-1/$\alpha_4\beta_7$ integrin interaction. The active con-

formation of compound **P10** is predictable based upon model peptides extensively investigated in our group and consists of two facing β-turns with the D-proline at the *i* + *1* position of a βII′-turn and the aspartic acid at the *i* + 1 position of βI- and/or βII-type. A systematic exchange of the amino acid residues maintaining the backbone structure resulted in several cyclic hexapeptides with improved activity (**P25**, **P28**−**P31**). The IC$_{50}$ values for these peptides are reported in Table 7. A linear peptide, which was described by Shroff et al. to inhibit $\alpha_4\beta_7$ integrin binding to MAdCAM-1 in the low micromolar range,[49] was measured for comparison. The high selectivity of these peptides was demonstrated by their potent inhibition of the $\alpha_4\beta_7$/MAdCAM-1 interaction, without interfering in the $\alpha_4\beta_1$/VCAM-1 binding. NMR data and molecular modeling simulations run for the potent compound **P25** confirmed our structural assumptions. Therefore, these results show the efficiency of the spatial screening strategy to develop potent and selective integrin inhibitors.

Experimental Section

Materials and Methods. All chemicals were used as supplied without further purification. Apart from *N*-methylpyrrolidone (NMP), all organic solvents were distilled before use. Fmoc amino acids were purchased from Bachem (Heidelberg, Germany). Tritylchlorid (Trt) resin was bought from Rapp Polymere (Tübingen, Germany), TBTU from Richelieu Biotechnologies (Montreal, Canada), and HOBt from Novabiochem (Läufelfingen, Switzerland).

Chemistry. The synthesis of the linear peptides was performed using solid-phase peptide synthesis[32,33] with Trt resin applying Fmoc strategy.[34] The Fmoc protected amino acids were coupled with *O*-(1*H*-benzotriazole-1-yl)-*N*,*N*,*N*,*N*-tetramethyluronium tetrafluoroborate (TBTU), 1-hydroxybenzotriazole (HOBt), and diisopropylethylamine (DIEA) as base in *N*-methypyrrolidone (NMP) as solvent. The full protected linear amino acid sequences were cleaved from the resin using a mixture of dichloromethane (DCM), trifluorethanol (TFE), and acetic acid 8:1:1. Cyclization of the linear sequences was carried out at high dilution in DMF (1.25×10^{-3} M) via in
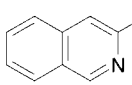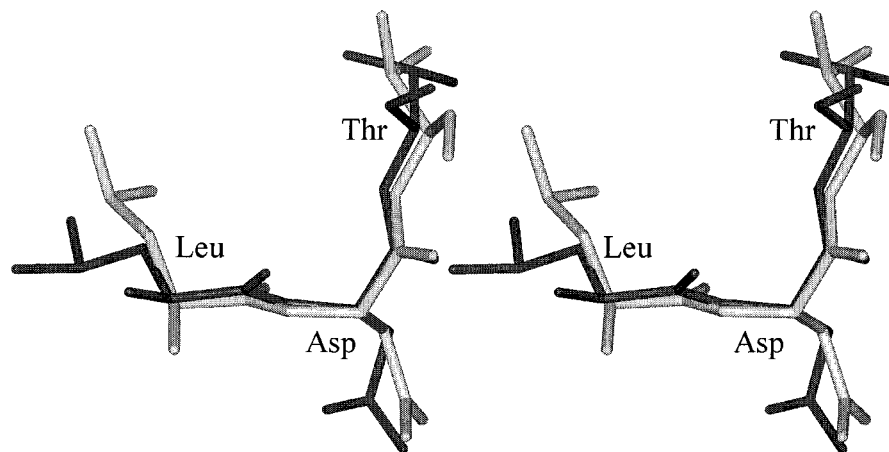
Figure 5. Stereoview of the superposition of the LDT sequence found in the X-ray structure of MAdCAM-Ig (gray) with the same sequence determined in solution for our potent peptide **P25** (black). Only C^α and C^β are considered for the RMSD calculation.

Table 7. IC_{50} Values of the Most Representative Cyclic Peptides for Inhibition of α₄β₇/MAdCAM Interactions[a]

Compound		IC50 (μM)
p25	*cyclo*(L-D-T-A-p-F)	292 ± 68
P28	*cyclo*(L-D-T-D-p-F)	163 ± 30
P29	*cyclo*(L-D-T-D-p-H)	301 ± 130
P30	*cyclo*(L-D-T-D-p-Y)	308 ± 18
P31	*cyclo*(L-D-T-D-p-M)	317 ± 116
Control[49] peptide	[isoquinoline]—CO-L-D-T-NH₂	465 ± 176

[a] The data represent the mean ±SD of at least three independent experiments.

situ activation using diphenyl phosphorazidate (DPPA) with sodium bicarbonate as solid base.[35] Final deprotection was achieved with trifluoroacetic acid (90% TFA) and scavengers (6% triisopropylsilane, 4% water). Purification by reversed phase high performance liquid chromatography (RP HPLC) yielded peptides which were >98% pure. The peptides were characterized by ESI mass spectroscopy and by 1D, 2D ^{1}H, ^{13}C NMR spectroscopy.[36]

NMR Spectroscopy. The spectra were acquired with Bruker DMX500 and DMX600 spectrometers in DMSO-d_6 as solvent and referenced relative to the residual DMSO signal (δ ^{1}H, 2.49 ppm; δ ^{13}C, 39.5 ppm). The assignment of all proton and carbon resonances was carried out using standard procedures.[36,37] Sequential assignment was accomplished by through bond connectivities from heteronuclear multibond correlation (HMBC)[39,40] spectra. Proton distances were calculated using the two spin approximation from rotating frame nuclear Overhauser enhancement (ROESY)[41,42] spectra. Homonuclear coupling constants were determined from one-dimensional spectra and from P.E.COSY[43] cross-peaks. The temperature coefficients for the amide protons were determined via ^{1}H spectra in the range from 300 to 315 K with a step size of 5 K.

Computer Simulations. The structure calculations were performed on Silicon Graphics computers. Metric matrix distance geometry (DG) calculations were carried out using a modified[44] version of DISGEO.[45,46] The DG procedure started with the embedding of 100 structures using random metrization.[47] For the refinement of the structures, DISGEO employs distance driven dynamics with all the ROE data restraints (inter- and intraresidue). The structure resulting from the DG calculation was used as the starting point for subsequent molecular modeling refinement. Energy minimization (EM) and MD calculations were carried out with the program DISCOVER using the CVFF[48] and a dielectric constant of 46.

After constrained EM using steepest descent and conjugate gradient, the system was heated gradually starting from 300 K up to 800 K and subsequently cooled to 300 K using at every temperature 5 ps steps. Configurations were saved every 25 ps for another 500 ps. During molecular modeling simuations only interresidual ROEs between backbone proton were taken into account. All the structures coming from MD simulations were mimimized without ROE constraints using again steepest descent and conjugate gradient algorithms.

Cell Adhesion Assay. CHO cells transfected with MAdCAM-1 (($2-3$) $\times$ 10⁴/well) were added to 96-well plates and allowed to grow for 24 h prior to the assay. Confluent cell monolayers were washed once with PBS and subsequently with adhesion assay buffer (24 mM Tris, pH 7.4, containing 137 mM NaCl, 2.7 mM KCl, 2 mM glucose, and 1% BSA). For adhesion assays with MAdCAM-Ig, 96-well plates were coated with donkey anti-human IgG (0.5 μg in 100 μL PBS/well) overnight at 4 °C. The plates were washed with adhesion assay buffer (Click's RPMI, 1% BSA, 1.0 mM Ca²⁺, 1.0 mM Mg²⁺) and incubated with 100 ng MAdCAM-Ig for 30 min at room temperature. After washing with adhesion assay buffer, the plates were blocked with adhesion assay buffer for 1 h at 37 °C. Alternatively, the plates were coated for 16 h at 4 °C with 400 ng/well VCAM-1 or 2 μg/well purified laminin in 50 mM carbonate buffer (pH 9.4). To the best of our knowledge, there is no evidence so far to assume that the results of inhibition experiments with antibodies or low molecular weight substances such as peptides would differ qualitatively between the two types of assays (cell–cell and plate assays). The plate assay using MAdCAM-Ig fusion proteins is often preferred, because it avoids "background problems" by nonrelated cell–cell adhesion structures.

38-β7 lymphoma cells,[10,13] Jurkat lymphoma cells, or human PBL were labeled for 30 min at 37 °C with 12 μg/mL H33342 dye (Calbiochem, LA Jolla, CA) in cell adhesion buffer and washed with PBS containing 1 mM EDTA and with PBS. The cells (8 $\times$ 10⁵ cells/mL) were resuspended in cell adhesion buffer containing 1.0 mM Ca²⁺ and 1.0 mM Mg²⁺. The cyclic peptides were preincubated with the cells at the final concentration of 1 mg/mL for 10 min at 37 °C. Subsequently, cells were allowed to adhere for 30 min at 37 °C, and nonadherent cells were removed by inverse centrifugation for 10 min at 50g. Adhesion assays were quantified by fluorimetry using a Cytofluor 2300 (Millipore, Bedford, MA).

References

(1) Hynes, R. O. Integrins: versatility, modulation, and signaling in cell adhesion. *Cell* **1992**, *69*, 11–25.

(2) Eble, J. A. Integrins — a versatile and old family of cell adhesion molecules. *Integrin-Ligand Interaction*; Springer-Verlag: Heidelberg, 1997; pp 1–40.

(3) Hemler, M. E. VLA proteins in the integrin family: structures, functions, and their role on leukocytes. *Annu. Rev. Immunol.* **1990**, *8*, 365–400.

(4) Postigo, A. A.; Sanchez-Mateos, P.; Lazarovits, A. I.; Sanchez-Madrid, F.; de Landazuri, M. O. Alpha 4 beta 7 integrin mediates B cell binding to fibronectin and vascular cell adhesion molecule-1. Expression and function of alpha 4 integrins on human B lymphocytes. *J. Immunol.* **1993**, *151*, 2471–2483.

(5) Berlin, C.; Berg, E. L.; Briskin, M. J.; Andrew, D. P.; Kilshaw, P. J.; et al. Alpha4beta7 integrin mediates lymphocyte binding to the mucosal vascular addressin madcam-1. *Cell* **1993**, *74*, 185–195.

(6) Kilger, G.; Holzmann, B. Molecular analysis of the physiological and pathophysiological role of alpha 4-integrins. *J. Mol. Med.* **1995**, *73*, 347–354.

(7) Shroff, H. N.; Schwender, C. F.; Dottavio, D.; Yang, L.-L.; Briskin, M. J. Small peptide inhibitors of alpha4beta7 mediated MAdCAM-1 adhesion to lymphocytes. *Bioorg. Med. Chem. Lett.* **1996**, *6*, 2495–2500.

(8) Briskin, M. J.; Rott, L.; Butcher, E. C. Structural requirements for mucosal vascular addressin binding to its lymphocyte receptor alpha4beta7. *J. Immunol.* **1996**, *156*, 719–726.

(9) Viney, J. L.; Joenes, S.; Chiu, H. H.; Lagrimas, B.; Renz, M. E.; et al. Mucosal addressin cell adhesion molecule-1. *J. Immunol.* **1996**, *157*, 2488–2497.

(10) Strauch, U. G.; Lifka, A.; Gosslar, U.; Kilshaw, P. J.; Clements, J.; et al. Distinct binding specificities of integrins alpha4beta7 (LPAM-1), alpha 4beta (VLA-4), and alpha IEL beta7. *Int. Immunol.* **1994**, *6*, 263–275.

(11) Holzmann, B.; McIntyre, B. W.; Weissman, I. L. Identification of a murine Peyer's Patch — specific lymphocyte homing receptor as an integrin molecule with an alpha chain homologous to human VLA-4 alpha. *Cell* **1989**, *56*, 37–46.

(12) Holzmann, B.; Weissman, I. L. Peyer's patch-specific lymphocyte homing receptors consist of a VLA-4 like alpha chain associated with either of two integrin beta chains, one of which is novel. *EMBO* **1989**, *8*, 1735–1741.

(13) Hu, M. C.; Crowe, D. T.; Weissman, I. L.; Holzmann, B. Cloning and expression of mouse integrin beta p(beta 7): a functional role in Peyer's patch-specific lymphocyte homing. *Proc. Natl. Acad. Sci. U.S.A.* **1992**, *89*, 8254–8288.

(14) Picarella, D.; Hurlbut, P.; Rottman, J.; Shi, X.; Butcher, E. et al. Monoclonal antibodies specific for beta 7 integrin and mucosal addressin cell adhesion molecule-1 (MAdCAM-1) reduce inflammation in the colon of scid mice reconstituted with CD45RBhigh CD4+ T cells. *J. Immunol.* **1997**, *158*, 2099–20106.

(15) Yang, X. D.; Sytwu, H. K.; McDevitt, H. O.; Michie, S. A. Involvement of beta 7 integrin and mucosal addressin cell adhesion molecule-1 (MAdCAM-1) in the development of diabetes in obese diabetic mice. *Diabetes* **1997**, *46*, 1542–1547.

(16) Haubner, R.; Finsinger, D.; Kessler, H. Stereoisomeric peptide libraries and peptidomimetics for designing selective inhibitors of the alphavbeta3 lntegrin for new cancer therapy. *Angew. Chem., Int. Ed. Engl.* **1997**, *36*, 1374–1389.

(17) Kessler, H. Conformation and biological activity of cyclic peptides. *Angew. Chem., Int. Ed. Engl.* **1982**, *21*, 512–523.

(18) Gurrath, M.; Müller, G.; Kessler, H.; Aumailley, M.; Timpl, R. Conformation/activity studies of rational designed anti-adhesive RGD peptides. *Eur. J. Biochem.* **1992**, *210*, 911–921.

(19) Aumailley, M.; Gurrath, M.; Müller, G.; Calvete, J.; Timpl, R.; et al. Arg-Gly-Asp constrained within cyclic pentapeptides. Strong and selective inhibitors of cell adhesion to vitronectin and laminin fragment P1. *FEBS Lett.* **1991**, *291*, 50–54.

(20) Matter, H.; Kessler, H. Structures, dynamics, and biological activities of 15 cyclic hexapeptide analogues of the alpha-amylase inhibitor Tendamistat (HOE 467) in solution. *J. Am. Chem. Soc.* **1995**, *117*, 3347–3359.

(21) Kessler, H.; Kutscher, B. Peptidkonformationen 40. Cyclische Hexapeptidanaloge des Thymopoietins. Synthese und Konformationsstudien. *Liebigs Ann. Chem.* **1986**, 914–931.

(22) Matter, H.; Gemmecker, G.; Kessler, H. Influence of serine in position i on conformation and dynamics of revers turns. *Int. J. Pept. Protein Res.* **1995**, *45*, 430–440.

(23) Richardson, J. S. The anatomy and taxonomy of protein structure. *Adv. Protein Chem.* **1981**, *34*, 167–339.

(24) Kurz, M. Cyclische Modellpetide als Template für ein konformationell orientiertes Peptiddesign. (Cyclic model peptides as templates for a conformational oriented peptide-design.) Ph.D. thesis, Technische Universität München, München, 1991.

(25) Riemer, C. Peptidomimetika und Strukturtemplate für die Anwendung im Design von Wirkstoffen. (Peptidomimetics and structure templates for drug design.) Ph.D. thesis, Technische Universität München, München, 1999.

(26) Mierke, D. F.; Kurz, M.; Kessler, H. Peptide flexibility and caculations of an ensemble of molecules. *J. Am. Chem. Soc.* **1994**, *116*, 1042–1049.

(27) Kessler, H.; Gemmecker, G.; Haupt, A.; Klein, M.; Wagner, K.; et al. Peptide conformations 47. Alanine containing analogues of cyclo(D-Pro-Phe-Thr-Lys(Z)-Trp-Phe-) — conformationally controlled structure–activity-relationships. *Tetrahedron* **1988**, *44*, 745–759.

(28) Komoriya, A.; Green, L. J.; Mervic, M.; Yamada, S. S.; Yamada, K. M.; et al. The minimal essential sequence for a major cell type-specific adhesion site (CS1) within the alternatively spliced type III connecting segment domain of fibronectin is leucine-aspartic acid-valine. *J. Biol. Chem.* **1991**, *266*, 15075–15079.

(29) Wayner, E. A.; Kovach, N. L. Activation-dependent recognition by hematopoietic cells of the LDV sequence in the V region of fibronectin. *J. Cell Biol.* **1992**, *116*, 489–497.

(30) Kessler, H.; Diefenbach, B.; Finsinger, D.; Geyer, A.; Gurrath, M.; et al. Design of superactive and selective integrin receptor antagonists containing the RGD sequence. *LIPS* **1995**, *2*, 155–160.

(31) Tan, K.; Casasnovas, J. M.; Liu, J. H.; Briskin, M. J.; Springer, T. A.; et al. The structure of immunoglobulin superfamily domains 1 and 2 of MAdCAM-1 reveals novel features important for integrin recognition. *Structure* **1998**, *6*, 793–801.

(32) Merrifield, R. B. Solid-phase peptide synthesis. *J. Am. Chem. Soc.* **1963**, *85*, 2149–2154.

(33) Merrifield, R. B. Solid-phase synthesis. *Angew. Che. Int., Ed. Engl.* **1985**, *24*, 799–810.

(34) Fields, G. B.; Noble, R. L. Solid-phase peptide synthesis utilizing 9-fluorenylmethoxycarbonyl amino acids. *Int. J. Pept. Protein Res.* **1990**, *35*, 161–214.

(35) Brady, S. F.; Palveda, W. J.; Arison, B. H.; Freidinger, R. M.; Nutt, R. F.; et al. Peptides '83: Structures and Function. *8th Ann. Pept. Symp.*; Pierce Chemical Company: Illinois, 1983; pp 127–130.

(36) Kessler, H.; Seip, S. NMR of peptides. In *Two-Dimensional NMR Spectroscopy: Applications for Chemists and Biochemists*; Croasmun, W. R., Carlson, R. M. K., Eds.; VCH Publishers: New York, 1994; pp 619–654.

(37) Kessler, H.; Schmitt, W. In *Encyclopedia of Nuclear Magnetic Resonance*; Grant, D. M., Harris, R. K., Eds.; J. Wiley & Sons: New York, 1996; Vol. 6, 3527–3537.

(38) Bax, A.; Summers, M. F. ^{1}H and ^{13}C Assignments from Sensitivity-Enhanced Detection of Heteronuclear Multiple-Bond Connectivity by 2D Multiple Quantum NMR. *J. Am. Chem. Soc.* **1986**, *108*, 2093–2094.

(39) Bermel, W.; Wagner, K.; Griesinger, C. Proton-Detected C,H Correlation via Long-Range Couplings with Soft Pulses; Determination of Coupling Constants. *J. Magn. Reson.* **1989**, *83*, 223–232.

(40) Kessler, H.; Schmieder, P.; Köck, M.; Kurz, M. Improved Resolution in Proton-Detected Heteronuclear Long-Range Correlation. *J. Magn. Reson.* **1990**, *88*, 615–618.

(41) Bothner-By, A. A.; Stevens, R. L.; Lee, J.; Warren, C. D.; Jeanloz, R. W. Structure Determination of a Tetrasaccharide: Transient Nuclear Overhauser Effects in the Rotating Frame. *J. Am. Chem. Soc.* **1984**, *106*, 811–813.

(42) Kessler, H.; Griesinger, C.; Kerssebaum, R.; Wagner, K.; Ernst, R. R. Separation of Cross-Relaxation and J Cross-Peaks in 2D Rotating Frame NMR Spectroscopy. *J. Am. Chem. Soc.* **1987**, *109*, 607–609.

(43) Mueller, L. P. E. COSY. A Simple Alternative to E. COSY. *J. Magn. Reson.* **1987**, *72*, 191–196.

(44) Mierke, D. F.; Kessler, H. Improved Molecular Dynamics Simulations for the Determination of Peptide Structures. *Biopolymers* **1993**, *33*, 1003–1017.

(45) Havel, T. F. DISGEO. Quantum Chemistry Exchange Program 1988, Exchange No. 507, Indiana Univeristy.

(46) Havel, T. F. An Evaluation of Computational Strategies for Use in the Determination of Protein Structure from Distance Constraints Obtained by Nuclear Magnetic Resonance. *Prog. Biophys. Mol. Biol.* **1991**, *56*, 43–78.

(47) Havel, T. F. The Sampling Properties of Some Distance Geometry Algorithms Applied to Unconstrained Polypeptide Chains: A Study of 1830 Independently Computed Conformations. *Biopolymers* **1990**, *29*, 1565–1585.

(48) Hagler, A. F.; Lifson, S.; Dauber, P. Consistent Force Field Studies of Intermolecular Forces in Hydrogen-Bonded Crystals. *J. Am. Chem. Soc.* **1979**, *101*, 5122–5130.

(49) Shroff, H. N.; Schwender, C. F.; Baxter, A. D.; Brookfield, F.; Payne, L. J.; Cochran, N. A.; Gallant, D. L.; Briskin, M. J. Novel modified tripeptide inhibitors of alpha4beta7 mediated lymphoid cell adhesion to MAdCAM-1. *Bioorg. Med. Chem. Lett.* **1998**, *8*, 1601–1606.

JM0005508